A Modal Concept for Active Noise Control in Circular or Annular Ducts

Ulf Tapken, Yanchang Zhang*, Lars Enghardt, Wolfgang Neise

DLR-Institut fuer Antriebstechnik, Abteilung Turbulenzforschung Berlin, Mueller-Breslau-Strasse 8, 10623 Berlin, Germany; *now with LUK GmbH & Co, Industriestrasse 3, 77815 Buehl, Germany

1. Introduction

Active control of sound propagation in ducts plays an important role in many technical applications, e.g. the attenuation of noise in ventilating systems or in the exhaust systems of combustion engines. Today many control strategies exist for the simplest case, which is the noise control in the low frequency range in ducts the lateral dimensions of which are small compared to the wavelength of sound. Up to the cut-on frequency of the first higher order mode a suppression of the propagating plane sound waves is possible in a broad frequency range.

The situation is more difficult when the lateral duct dimensions become large compared to the wavelength, as for example in the intake section of an aircraft engine. With increasing rotor speed an increasing number of acoustical modes becomes present. This means, the system comprises an increasing number of degrees of freedom. As a consequence, control of the sound field is practicable just in a narrow frequency band or even limited to discrete frequencies.

In figure 1 the frequency spectrum of the sound field in the duct section of a turbo-machine is depicted. Obviously the fan produces tones of high intensity compared to the broad band noise level. Attenuation of these tones by means of passive absorbers often is not sufficient. Therefore the active suppression of the tones represents a reasonable improvement.

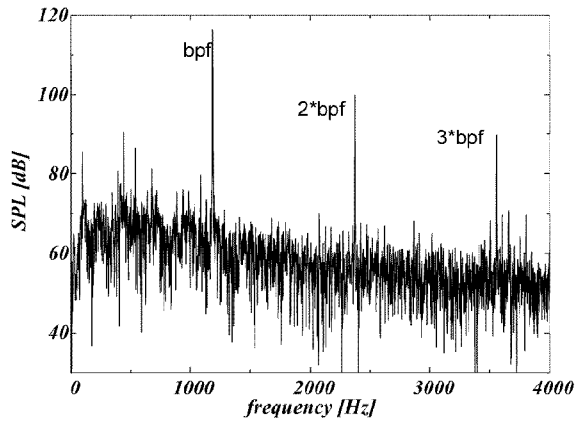

Figure 1: Sound pressure spectrum detected by a microphone in the duct section of a turbo-machine (bpf=blade passing frequency).

A common approach for active noise control consists in the use of the well known adaptive LMS-algorithm. This strategy ignores to a certain extent the properties of the physical system to be controlled. Furthermore, with increasing complexity of the modal sound field the numerical costs of the adaptive system increase fast and the problem of numerical instabilities occurs. Thus a physical approach is reasonable, which aims at minimisation of only the dominant modes of the undesired tone. This results in a reduction of the control effort. Furthermore the stability of the complete modal control process is improved due to its separation into a number of independent subprocesses for individual modes. Besides, as another control strategy, the directivity of the radiated tones in the far field outside the duct can be influenced through a specific control of the modal structure.

In this regard a azimuthal mode control strategy was developed and experimentally proved by NASA Lewis Research Centre in 1996 (Pla and Hu [1]). By use of a single ring with pressure sensors and one ring with actuators they were able to reduce one dominant azimuthal mode at the axial ring location of the sensors.

As the amplitude of the azimuthal mode is a function of the axial and the radial position in the duct, control at a single axial ring position does not ensure minimisation of that azimuthal mode at other duct positions, in particular if the sound wave has a high radial content.

A direct radial mode control strategy at present seems to be impossible in practice, because variations of temperature, frequency and flow velocity in the duct strongly influence the

Paper presented at the RTO AVT Symposium on "Active Control Technology for Enhanced Performance Operational Capabilities of Military Aircraft, Land Vehicles and Sea Vehicles", held in Braunschweig, Germany, 8-11 May 2000, and published in RTO MP-051.

accuracy of the online radial mode analysis. Besides, a large number of variables must be considered by the control system, leading to instabilities in the minimisation process.

Therefore, an improved control strategy has been proposed by Zhang et al: the indirect radial mode control (IRMC), which enables effective control of the modal sound field without directly determining the radial amplitudes. The method is based on the well-defined relationship between the azimuthal amplitudes at different axial positions, which is given implicitly by its composition of a fixed number of radial components. If one succeeds in reproducing the azimuthal amplitude and thus the correct linear superposition of radial components at different axial positions, suppression can be achieved not only at this distinct locations but also in the whole duct.

In the following chapters it will be shown, that the performance of the modal control strategy strongly depends on the proper choice of the number as well as the locations of the sensors and actuators.

2. The sound field description in circular and annular ducts

The propagation of sound pressure waves in cylindrical or annular ducts in the presence of uniform mean flow can be described by a linear acoustic wave equation, see e.g. [2]. A solution of the wave equation in cylindrical coordinates (x,r,φ) is given by a mathematical decomposition into azimuthal and radial components. In the frequency domain it can be written as (see [3]):

$$\tilde{p}(x,r,\varphi,\omega) = \sum_{m=-\infty}^{\infty} A_m(x,r,\omega)\cdot e^{im\varphi} \qquad (1)$$

$$A_m(x,r,\omega) = \sum_{n=0}^{\infty} f_{mn}(\sigma_{mn}\frac{r}{r_a})\left[A_{mn}^{-}(\omega)e^{ik_{mn}^{+}x} + A_{mn}^{-}(\omega)e^{ik_{mn}^{-}x}\right] \qquad (2)$$

where $A_m(x,r,\omega)$ is the amplitude of the azimuthal mode of order m. $A_m(x,r,\omega)$ expands into a series of radial modes with amplitudes $A_{mn}^{+}(\omega)$ and $A_{mn}(\omega)$. "+" denotes wave propagation in flow direction, "-" against flow dirction. $k_{mn}^{+}(\omega)$ and $k_{mn}^{-}(\omega)$ are the respective axial wavenumbers, r_a is the outer duct radius, and f_{mn} denotes the cylinder functions which describe the radial distribution of the modal sound pressure field in the circular or the annular duct (a detailed description can be found in [3]).

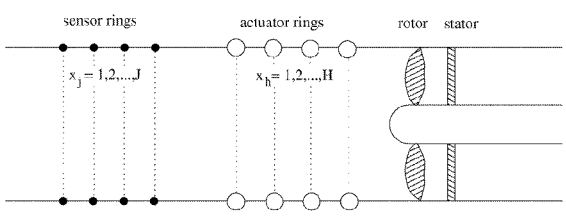

Figure 2: Longitudinal section of the duct.

3. The Indirect Radial Mode Control (IRMC)

In figure 2 the intake of a turbo machine is depicted with a sensor and an actuator array mounted flush with the inner duct wall. The sensors and actuators are arranged in several axial rings. In each ring the sensors resp. actuators are spaced evenly in the azimuthal direction φ. The number of sensors and actuators per ring must be chosen according to the Nyquist theorem. The arrangement of the sensors allows a azimuthal mode analysis for each ring as was demonstrated in [4]. It is a prerequisite for the IRMC-method processed in the azimuthal mode domain. Figure 3 gives an overview on the required signal processing.

With the azimuthal modal analysis realised as a real time application (see Böhning et al [5]) the modal amplitude $P_m(x_j,r_a,\omega)$ for each azimuthal mode order -m, ..., +m of the primary sound wave (produced by the rotor) can be determined for the set of sensor rings $\{x_j\}$. The objective of the IRMC is to cancel the azimuthal modes $P_m(x_j,r_a,\omega)$ by a secondary wave of adequate azimuthal mode amplitudes $S_m(x_j,r_a,\omega)$, which are generated by the actuators. Mathematically this is equivalent to minimisation of the sum of these mode amplitudes over all axial positions of the sensor rings, seperately for each azimuthal order m:

$$I_m(\omega) = \sum_{j=1}^{J}\left|P_m(x_j,r_a,\omega) + S_m(x_j,r_a,\omega)\right|^2 = Min. \qquad (3)$$

The secondary mode amplitude at the sensor locations $\{x_j\}$ generated by the actuators is given by

$$S_m(x_j,r_a,\omega) = \sum_{h=1}^{H}(t_m)_{hj}(\omega)\cdot\xi_m(x_h,r_a,\omega), \qquad (4)$$

where $\xi_m(x_h,r_a,\omega)$ represents the azimuthal mode amplitude of the actuator ring at the axial position x_h. $(t_m)_{hj}$ is the coefficient of the modal transfer matrix $\underline{\underline{T}}_m^{hj}$ which describes the modal transfer functions between the axial positions $\{x_h\}$ and $\{x_j\}$. The modal transfer matrix has to be determined in a separate step prior to application of ANC, see chapter 4.

From equation (2) it can be deduced, that in order to control an

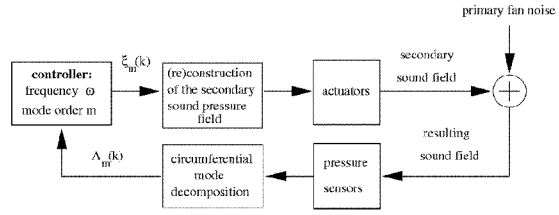

Figure 3: Schematic of the signal processing for IRMC.

azimuthal mode consisting of N radial modes, at least N sensor rings are necessary. If the azimuthal mode amplitude $P_m(x_j, r, \omega)$ at these N axial positions x_j is reproduced on the duct wall ($r = r_a$), the radial structure in the duct is also reproduced implicitly.

For simplicity a vector of azimuthal mode amplitudes of mode order m at the set of axial positions $\{x_j\}$ resp. $\{x_h\}$ is introduced:

$$\underline{P}_m := [P_m(x_1, r_a, \omega), P_m(x_2, r_a, \omega), ..., P_m(x_J, r_a, \omega)]^t,$$
$$\underline{S}_m := [S_m(x_1, r_a, \omega), S_m(x_2, r_a, \omega), ..., S_m(x_J, r_a, \omega)]^t,$$
$$\underline{\xi}_m := [\xi_m(x_1, r_a, \omega), \xi_m(x_2, r_a, \omega), ..., \xi_m(x_H, r_a, \omega)]^t. \quad \textbf{(5)}$$

In equ.(5) single tones with constant frequencies ω are considered. Since only wall-flush mounted sensors and actuators are used, r_a can be dropped in the further analysis. Thus equation (4) can be rewritten as

$$\underline{S}_m = \underline{\underline{T}}_m^{hj} \cdot \underline{\xi}_m, \quad \textbf{(6)}$$

and one obtains the solution of equation (3) as least square fit expression

$$\underline{\xi}_m = -((\underline{\underline{T}}_m^{hj})^{t*} \cdot \underline{\underline{T}}_m^{hj})^{-1} \cdot (\underline{\underline{T}}_m^{hj})^{t*} \cdot \underline{P}_m. \quad \textbf{(7)}$$

Since the system is linear, the control process can be performed separately for each mode order m of a single tone.

The final actuator signals (in the frequency domain) can be computed according to equation (1) for each actuator at position (x_h, r_a, φ_l). In order to generate the secondary tone with the correct phase leading to the cancellation of the primary field, it is locked to a trigger signal, which is produced by the rotor.

Theoretically the system of linear equations (7) can be solved exactly. In practice the inversion of the included hermitian matrix may be critical numerically and lead to instabilities. The problems that appear in connection with a matrix inversion will be discussed in more detail in chapter 5.

4. Simulation of the IRMC

Before performing IRMC the modal transfer matrix $\underline{\underline{T}}_m^{hj}$ has to be determined by an azimuthal mode transfer function measurement for each azimuthal mode order -m ,..., +m. The transfer matrices include the acoustical transfer path as well as the electro-mechanical transfer characteristics of the actuators and the respective signal processing. For the numerical simulation and analysis of the IRMC here the modal transfer matrix $\underline{\underline{T}}_m^{hj}$ is determined theoretically.

In order to get a more realistic azimuthal modal spectrum as an input for the simulation, a modal noise amplitude appropriate to a measurement error of the sensors is added to the modal amplitudes in $\underline{P}_m(\omega)$. The magnitude of the noise amplitude is related to the maximum modal amplitude by considering a given 'signal-to-noise-ratio' σ.

In figure 4 the simulation of the IRMC in the azimuthal mode domain is divided into two parts. In the first step the modal vector $\underline{P}_m$ is used to calculate the actuator signal amplitudes $\underline{\xi}_m$ according to equation (7). For brevity the corresponding transformation is represented by the modal transfer matrix $\underline{\underline{T}}_m^{jh}$ in figure 4. Equation (6) gives the secondary modal amplitudes $\underline{S}_m$ generated at the sensor locations with help of the modal transfer matrix $\underline{\underline{T}}_m^{hj}$. The residual amplitudes $\underline{E}_m$ are the result of the superposition of the primary and the secondary tone.

The presence of noise leads to deviations between the "measured" and the actual modal amplitudes at each sensor location,

$$E_m(x_j) = P_m(x_j) + S_m(x_j)$$
$$= P_m(x_j) + \sum_{h=1}^{H} (t_m)_{hj} \cdot \xi_m(x_h) \geq 0. \quad \textbf{(8)}$$

For that reason an iterative algorithm is used in the following steps, which should optimise the actuator amplitudes step by step in order to minimise the residual mode amplitude.
The task is solved by a multiple-channel LMS-algorithm in the azimuthal mode domain. The iterative algorithm, originally

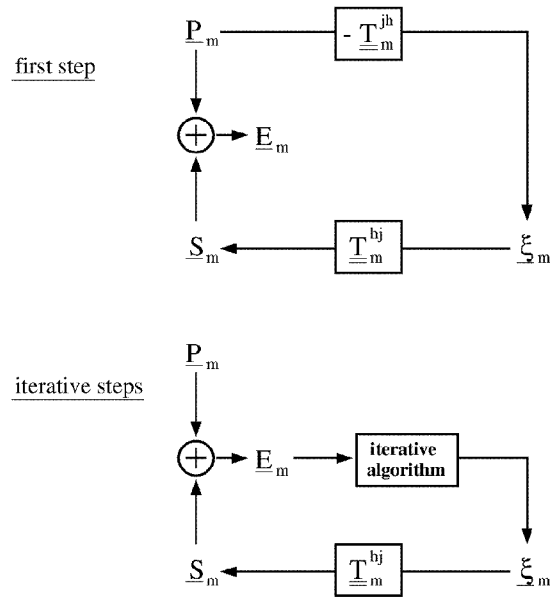

Figure 4: Initial and iterative steps implemented in the IRMC algorithm in the azimuthal mode domain.

designed for use in the frequency domain (see Kuo and Morgan [6]), minimises the residual mode amplitude according to equation (3) and gives the update prescription of the modal actuator vector for step n as

$$\underline{\xi}_m(n+1) = \underline{\xi}_m(n) + \mu \cdot (\underline{\underline{T}}_m^{hj})'^* \underline{E}_m(n), \qquad (9)$$

where μ is the adaptive step size parameter.

If all parameters of the sound field, i.e. frequency, temperature and mean flow velocity, are constant in time, then the spatial structure of the sound waves in the duct repeats periodically. Thus, since the actuator amplitudes are set in relationship to the trigger of the rotor, there is no need to process the iterative algorithm in real time.

In fact, calculation of the initial modal actuator amplitudes $\underline{\xi}_m(0)$ in the first step of the iterative algorithm is not mandatory, however, it leads to a faster convergence of the iterative process.

5. Analysis of the modal transfer matrix

In theory, without additional noise, the modal actuator signal amplitudes given in equation (7) should produce a cancelling tone $\underline{S}_m$ that exactly eliminates the primary tone $\underline{P}_m$. However, this is true only for azimuthal modes with a low radial content, which is equivalent to a corresponding modal transfer matrix of low rank. In this chapter it will be shown, that with increasing radial mode order n numerical restrictions lead to limitations with regard to the solution, which is exact analytically.

All calculations presented in this paper have been carried out for the configuration depicted in figure 2. A uniform flow of M=0.3 and equally spaced rings in the axial direction of the duct are assumed for various parameters $k_0 r_a$ (k_0 denotes the wavenumber for free field propagation). The axial distance between two consecutive rings is denoted by δx.

Calculation of the modal transfer matrix $\underline{\underline{T}}_m^{hj}$ involves the inversion of a hermitian matrix, named $\underline{\underline{U}}_m$ in the following. The accuracy of the modal transformation process strongly depends on the condition of $\underline{\underline{U}}_m$, whereby a low condition corresponds to a transformation with good accuracy. In other words, the condition of $\underline{\underline{U}}_m$ is a measure for the quality of the detection of the modes at the specified positions. Thus by an analysis of $\underline{\underline{T}}_m^{hj}$ resp. $\underline{\underline{U}}_m$, the optimum positioning of the sensors and actuators for application of the IRMC-technique can be examined.

In figure 5 the variation of the condition of $\underline{\underline{U}}_m$ with ring distance δx is shown for all propagating azimuthal mode orders and for three different values $k_0 r_a$. Obviously, the lower the mode order m the smaller the intervals of δx with a low condition are. This can be explained by the fact, that the lowest mode order m=0 has the largest radial content; see for illustration figure 6, where the normalised axial wavelengths of all propagating modes (m,n) are depicted for $k_0 r_a$ =16.3. For a low mode order m the differences between the corresponding axial wavelengths $\lambda_{mn}^{\pm}$ (n=0,...,N) become smaller, which makes the implicit modelling of the radial modes by the mathematical mapping more difficult. Furthermore the complexity of this problem increases with increasing $k_0 r_a$. On the other hand, axial ring

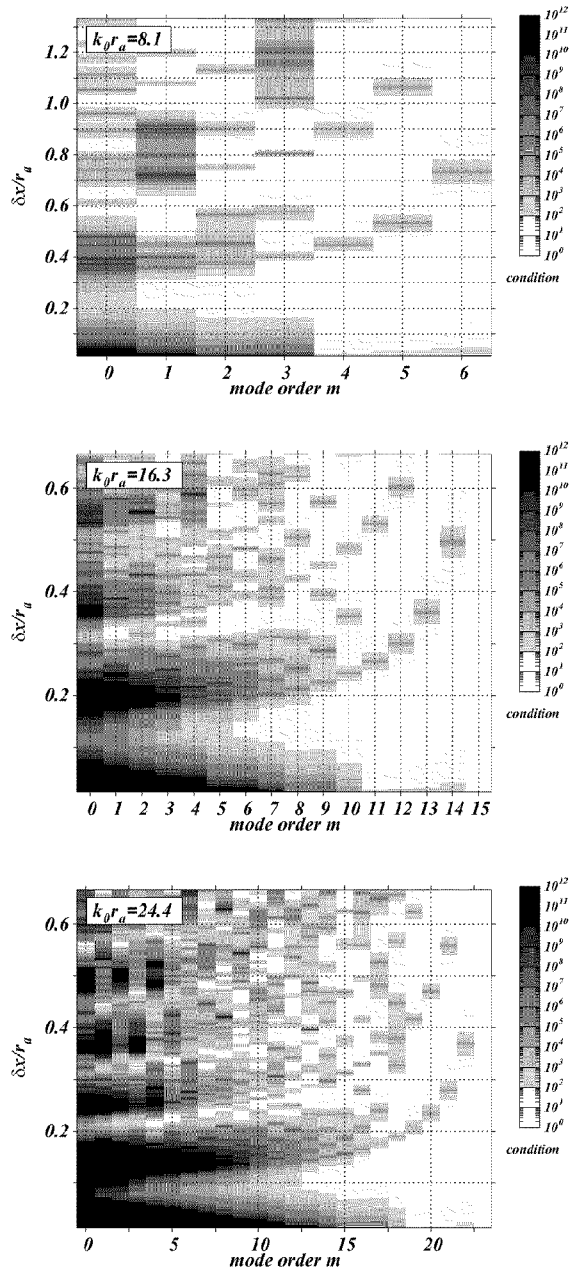

Figure 5: Condition of the hermitian matrix U_m as function of the axial ring spacing δx calculated for all propagating mode orders m and different values $k_0 r_a$.

spacing is almost arbitrary when the azimuthal mode order m is large and the radial mode content low.

In general, it is the lower mode order m that impose the essential restrictions with regard to the positioning of the rings. Comparison of the examples, shown in figure 5 leads to the conclusion, that for simultaneous control at several frequencies, the proper choice of the ring positions becomes a critical issue.

6. Analysis of the IRMC-Algorithm

The performance of the IRMC-algorithm in the presence of noise is examined in this chapter. The calculations have been carried out for the same parameters as in chapter 5 for $k_0 r_a = 16.3$. The magnitude of the amplitudes of the primary modes, that are radiated by the rotor and propagate upstream, are randomly distributed about $P_{mn}^{-} = 85$ dB. The reflected modes propagating in flow direction are assumed to be in the range of $P_{mn}^{+} = 70$ dB. The iterative control system is considered to be converged, if the mean residual amplitude over all sensors equals 50 dB.

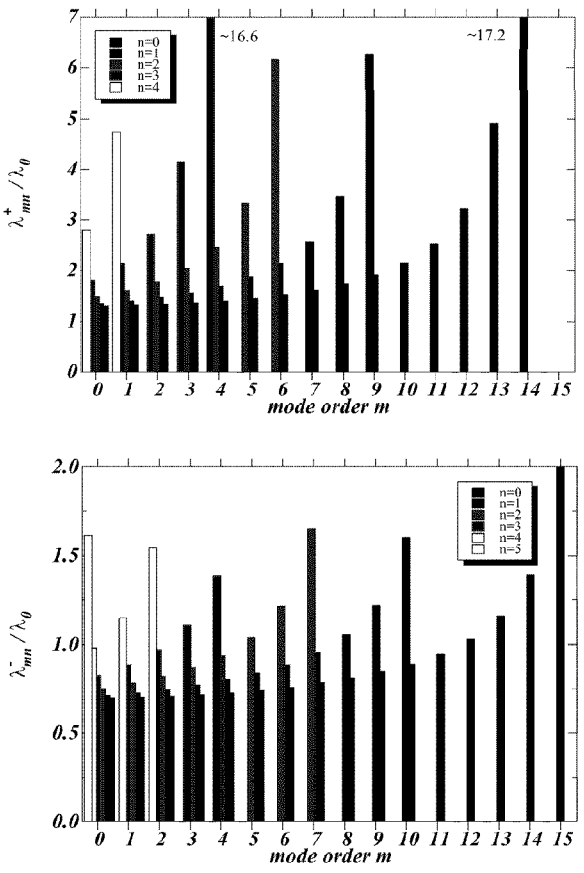

Figure 6: Normalized axial wavelengths λ^{+}_{mn} and λ^{-}_{mn} of the modes (m,n) propagating in resp. against flow direction for $k_0 r_a = 16.3$.

As pointed out in chapter 5, a system with an ill-conditioned transfer matrix is very sensitive to small disturbances of the input vector. This is confirmed by figure 7, which shows the number of iterations until convergence of the iterative algorithm depending on the axial ring spacing δx. The calculations are performed for mode order m=8 and different noise levels, given by the modal signal to noise ratio σ. The larger the disturbances, the larger the deviations between the calculated output of the modal matrix transform and the optimal solution, as it is described by equation (8). In the absence of noise or with very low noise levels (σ >30dB), the IRMC cancels the primary tone completely after the first step for any δx. For σ <30dB and a ring distance δx corresponding to a quite good condition, the control is stable and after a few iterations the algorithm also converges. But with increasing noise level, and ring spacings corresponding to an ill-conditioned system, the system becomes unstable. In these cases lots of iterations are necessary until convergence is reached, or the control system even does not converge at all.

In Figure 8 a control attempt for the mode order m=8 and an optimal ring spacing δx is shown for σ −5dB in comparison with σ −30dB. In the coordinate system used here, the rotor is located at x=0 and the uniform flow goes in the positive axial direction. Depicted are the magnitudes of the complex azimuthal mode amplitudes over the duct axis after the iterative algorithm has converged. Obviously the actuators reproduce the primary mode well, resulting in the cancellation of $\underline{P}_m$. The residual mode amplitude $\underline{E}_m$ strongly depends on the uncertainty of the measured azimuthal mode amplitudes.

The contour plot in figure 9 shows the residual modal ampli-

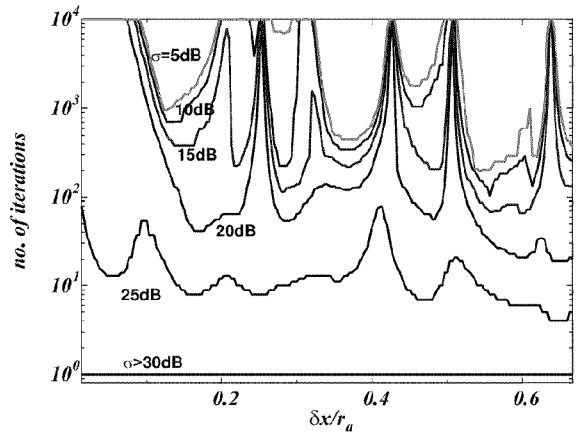

Figure 7: Number of iterations until convergence as a function of the sensor ring spacing for various modal signal to noise ratios σ (m=8, n=0,1, $k_0 r_a = 16.3$).

tudes $E_m(x, r_a)$ along the duct axis for the mode order m=8 and σ =15 dB for different ring spacing δx. As examination of the matrix $\underline{\underline{U}}_m$ predicted, for a ring spacing δx connected with bad condition of $\underline{\underline{U}}_m$, the system does not cancel the primary mode or even diverges, which is indicated by residual modal amplitude E_m larger than the modal amplitude P_m of the primary tone.

Note, that control of the primary mode at the locations of the sensors is successful for arbitrary ring spacings δx: the reduction at the axial positions of the sensor rings are clearly visible in the contour plot as white lines (the arrows mark the moving positions of the rings with increasing δx). The important conclusion is, that a control observed at the sensors does not necessarily mean a reduction of the primary mode in the entire duct.

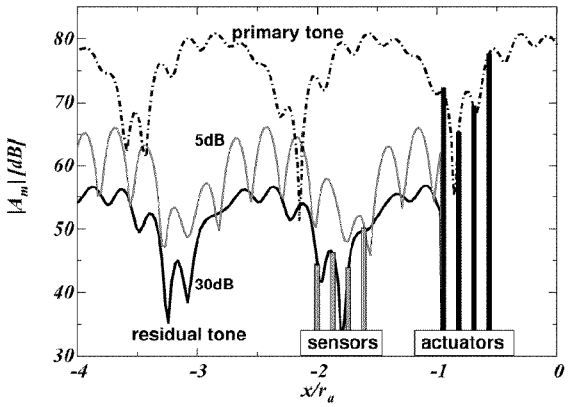

Figure 8: Azimuthal mode amplitude of the primary and the residual tone along the duct axis for modal signal to noise ratios of σ =5 and 30 dB after convergence of the IRMC (m=8, n$^{\pm}$=0,1, $k_0 r_a$ = 16.3, rotor at x=0).

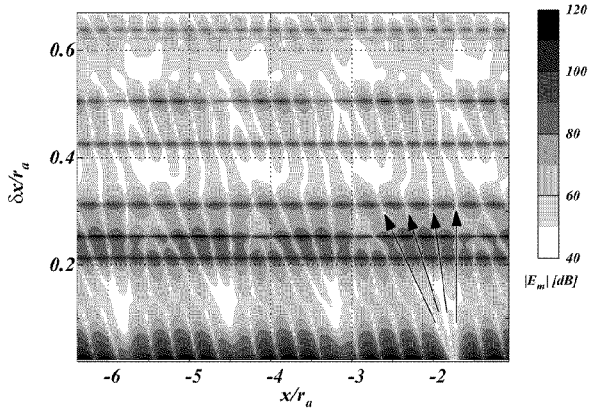

Figure 9: Residual azimuthal mode amplitude along the duct axis with a modal signal to noise ratio of σ =15 dB; the arrows mark the positions of the sensor rings depending on δx (m=8, n$^{\pm}$=0,1, $k_0 r_a$ = 16.3, rotor at x=0).

The upper graph of figure 10 shows a control attempt for mode order m=1 and σ =25dB. The azimuthal mode contains 10 radial modes (cp. figure 6) and should be detected by 10 sensor rings with an axial spacing $\delta x / r_a = 0.1$ corresponding to a matrix $\underline{\underline{U}}_m$ with minimum condition. Nevertheless the condition for this configuration is quite bad and convergence is not reached. This example again confirms, that control achieved at the sensor location does not imply control at all duct locations. The situation is improved with additional sensor inputs, e.g. with 13 sensors, which is shown in the bottom graph of figure 10. The corresponding matrix $\underline{\underline{U}}_m$ still is bad conditioned. However, if the inverting process of the hermitian matrix is carried out via a singular value decomposition, columns corresponding to singular values close to zero can be rejected, which results in an improved condition and performance of the IRMC.

Since the IRMC-technique makes use of wall flushed sensors and actuators, one has to prove that not only the modal amplitudes at the duct wall are controlled but also the whole azi-

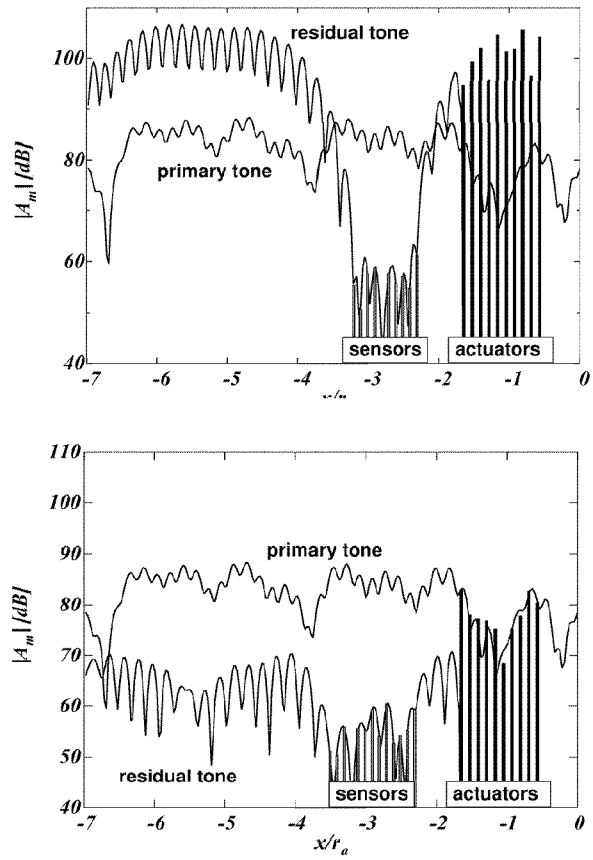

Figure 10: Azimuthal mode amplitude of the primary and the residual tone along the duct axis for a modal signal to noise ratio of 25 dB and 10 sensor rings (top) resp. 13 sensor rings (bottom) (axial ring spacing $\delta x / r_a$ = 0.1, m=1, n$^{\pm}$=0,...,4, $k_0 r_a$ = 16.3, rotor at x=0).

muthal and radial structure across the duct. Evidence to that regard is given in figure 11 and 12, which show the pattern of the primary and residual azimuthal mode, $\underline{P}_m$ and $\underline{E}_m$ resp., across the duct corresponding to the control attempt shown in figure 10.

7. Summary

The results of the analysis and simulation show, that the IRMC-concept enables an effective control of the azimuthal and radial structure of acoustical modes in circular and annular ducts without the need to determine the radial amplitudes directly. All azimuthal modes of a tone can be reduced by using the same ring spacing for the sensor rings and actuator rings. In this context, the lower azimuthal mode orders m impose the most stringent requirements for the axial spacing. For effective control of an azimuthal mode m with a high radial content (N radial modes), more than N sensor rings are necessary. Control attempts at several frequencies simultaneously require a detailed analysis with respect to the optimal ring spacing.

An important result with regard to the experimental analysis of active control concepts is, that noise control achieved at the positions of the sensors does not necessarily mean a complete control at all positions in the duct.

The simulation results show further, that it is not necessary to place the sensor rings in the axial direction according to a spatial Nyquist criterion. This can be explained by the fact, that in the adaptation process only the radial mode amplitudes belonging to certain discrete modal wavenumbers $k_{mn}^{\pm}$ have to be fitted implicitly.

Another result is, that complete control is possible in the duct although the sensor array covers less than half of the maximum modal wavelength.

In future investigations non equidistant axial spacing of the rings has to be examined with respect to matrices with improved conditions. Additionally improved methods for matrix inversions have to be tested. A perturbation method may give more information in this context.

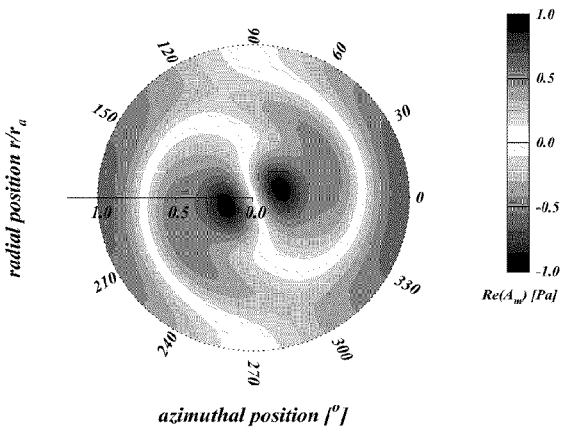

Figure 11: Pattern of the azimuthal mode amplitude (mode order m=1) of the primary tone in the cross section of the duct at x/r_a =-4.5 (parameters as in figure 10).

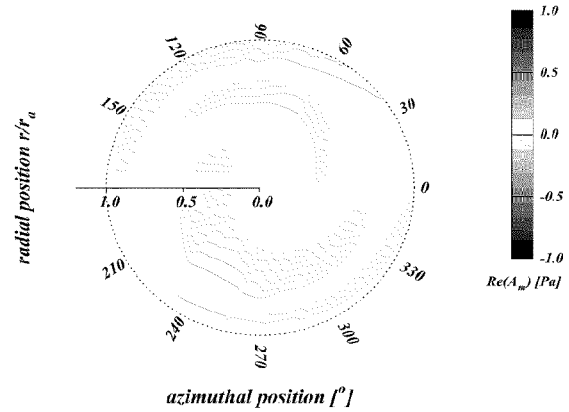

Figure 12: Pattern of the azimuthal mode amplitude (mode order m=1) of the residual tone in the cross section of the duct at x/r_a =-4.5 (parameters as in figure 10).

8. References

[1] Pla, F.G.; Hu, Z.: Active Control of Fan Noise: Feasibilty Study, Volume 3: Active Fan Noise Cancellation in the NASA Lewis Active Control Fan Facility, NASA Contractor Report NAS3-26617, September 1996

[2] Munjal, M.L.: Acoustics of ducts and mufflers; John Wiley & Sons, 1987

[3] Holste, F.; Neise, W.: Noise Source Identification in a Propfan Model by Means of Acoustical Near Field Measurements, Journal of Sound & Vibration, 203(4), pp. 641-665, 1997

[4] Enghardt, L.; Zhang, Y.; Neise, W.: Experimental verification of a radial mode analysis technique using wall-flush mounted sensors; Forum Acusticum – integrating the 25th German Acoustic DAGA Conference, Berlin March 1999, ISBN 3-9804568-5-4

[5] Böhning, P.; Enghardt, L; Neise, W; Költzsch, P.: Entwicklung einer Software zur Kurzzeit-Azimutalmodenanalyse; DAGA 2000, Oldenburg March 2000 - Fortschritte der Akustik (Proc. Annual Meeting of the German Acoustical Society, to be published)

[6] Kuo, S.M.; Morgan, D.R: Active Noise Control Systems, Wiley-Interscience Publ., 1996

This page has been deliberately left blank

Page intentionnellement blanche